Vol 15 No 11, November 2006
1009-1963/2006/15(11)/2583-05
Chinese Physics
© 2006 Chin. Phys. Soc.
and IOP Publishing Ltd

The influence from high-n dielectronic satellites to Kα resonance line in helium-like aluminium*

Fu Yan-Biao (符彦飙)[a], Dong Chen-Zhong (董晨钟)[a]†, Zhang Deng-Hong(张登红)[a], Koike Fumihiro (小池文博)[b], and Kato Takako(加藤隆子)[c]

[a] *College of Physics and Electronic Engineering, Northwest Normal University, Lanzhou* 730070, *China*
[b] *Physics Department, School of Medicine, Kitasato University,* 1-15-1 *Kitasato* 228-8555, *Japan*
[c] *Atomic and Molecular Data Research Center, National Institute for Fusion Science, Toki* 509-5292, *Japan*

(Received 25 March 2006; revised manuscript received 19 May 2006)

Based on the multi-configuration Dirac–Fock method, this paper has made theoretical calculations for the dielectronic recombination cross-sections and the high-n dielectronic satellites to Kα resonance line in helium-like aluminium ions. It is found that high-n dielectronic satellites are seriously mixed with resonance line, which leads to a significant increase in both the apparent width and the intensity of Kα resonance line. They also induce a positional shift of Kα resonance line.

Keywords: dielectronic satellites, dielectronic recombination, resonance line
PACC: 3480L

1. Introduction

When a 2p-shell electron undergoes radiative transitions to 1s-shell, we have Kα resonance line. The Kα resonance line is a characteristic line for various elements. It is extensively used for determining the parameters of high-temperature tokamak plasmas.[1−3] But the line is often blended with lithium-like dielectronic satellites (DS) due to transitions $1s^2nl - 1s2pnl$ with $n \geq 3$. These satellites give a significant increase in both the apparent width and the apparent intensity of the resonance line. They also influence the evaluation of the satellite-to-resonance-line ratio for diagnostics of solar flares and tokamak plasmas.[4] On the other hand, as originally pointed out by Nardi and Zinamon,[5] Kα satellite lines can be used to diagnose plasma conditions in energetic particle beam experiments. In target ions with partially filled L-shells, the Kα satellite lines exhibit a detectable shift to shorter wavelengths as the number of L-shell spectator electrons decreases. Thus, the wavelength of the emission reflects the target ionization stage. This feature has also been used to investigate hot electron transport in laser-produced plasmas,[6,7] where the K-shell vacancies are produced by the hyper-thermal electrons. For these diagnostics applications, the study of the satellites is indispensable, one has to determine the contribution of these satellites to the Kα resonance line as accurate as possible.

Although the main abundance is from hydrogen and helium in cosmic cloud, the study of other elements such as Al, Mg, Fe is also important and has become well feasible in the couple of decades.[8] The DS from lithium-like aluminium has been studied both experimentally and theoretically,[9,10] but there is no particular study of high-n DS from lithium-like aluminium as far as we find in the literature. In this paper, we present a detailed analysis of high-n dielectronic satellites from lithium-like aluminium by using the dielectronic recombination program[11] which we developed recently based on the multi-configuration Dirac–Fock method. The contributions of the satellites to Kα resonance will be discussed. In the practical calculations, the high-n contributions from $n = 3$ to 10 is evaluated directly, and the results are extrapolated up to $n = 100$. A comparison of the present theory with experiments will be an issue in coming papers.

2. Theoretical method

The DS transition processes of helium-like aluminium has a form

*Project supported by the National Natural Science Foundation of China (Grant Nos 10376026 and 10434100), and the Foundation of Center of Theoretical Nuclear Physics of National Laboratory of Heavy Ion Accelerator of Lanzhou, China.
†Corresponding author. E-mail: dongcz@nwnu.edu.cn

$$\begin{aligned} e^- + Al^{11+}(1s^2) &\rightarrow Al^{10+}(1sn_rl_rnl)^{**} \\ &\rightarrow Al^{10+}(1s^2nl)^* + h\nu\,. \end{aligned} \quad (1)$$

A free electron collides with an ion $Al^{11+}(1s^2)$ (denoted as i from now on) and it is captured into a nl orbital after exciting one electron in 'i' into an n_rl_r orbital, resulting with the formation of a resonant doubly excited state $Al^{10+}(1sn_rl_rnl)^{**}$ (denoted as j from now on). This process is followed by a radiative decay of 'j' into the state $Al^{10+}(1s^2nl)^*$ (will be denoted as k from now on), providing us with DS lines. The DS cross-section from i to k through j can be given by the following equation in the framework of two step approximation:

$$\sigma_{\rm DS}(i,j,k) = \sigma^{\rm c}_{i,j} B^{\rm r}_{j,k}, \quad (2)$$

where $\sigma^{\rm c}_{i,j}$ is the cross-section of the resonant capture process from $i \rightarrow j$, and $B^{\rm r}_{j,k}$ is the radiative branching ratio for the process from j to k. The quantities $\sigma^{\rm c}_{i,j}$ and $B^{\rm r}_{j,k}$ can be calculated by[4]

$$\sigma^{\rm c}_{i,j} = \frac{\pi^2\hbar^3}{m_{\rm e}\varepsilon_j}\frac{g_j}{2g_j}A^{\rm a}_{ji}\delta(\varepsilon-\varepsilon_j), \quad (3)$$

and

$$B^{\rm r}_{j,k} = \frac{A^{\rm r}_{jk}}{\Sigma_{k'}A^{\rm r}_{jk'} + \Sigma_{i'}A^{\rm a}_{ji'}}, \quad (4)$$

where g_i and g_j are the statistical weights of the state i and j respectively, the summation i' runs over all the possible Auger final states, the summation k' runs over all the possible radiative final states and $\delta(\varepsilon-\varepsilon_j)$ is a delta function that requires the matching of the free electron energy ε to the resonance state energy ε_j. The radiative decay rate $A^{\rm r}_{jk}$ is given by[12]

$$A^{\rm r}_{jk} = \frac{4e^2\omega_p}{3\hbar c^3 g_j}|\langle\Psi_j|T^{(t)}|\Psi_k\rangle|^2, \quad (5)$$

where Ψ_j and Ψ_k are atomic state function (ASF) for the states j and k respectively, ω_p is the photon energy, and $T^{(\rm t)}$ is a multipole radiative tensor operator. And the Auger decay rate $A^{\rm a}_{ji}$ is given by[13]

$$A^{\rm a}_{ji} = \frac{2\pi}{\hbar}\left|\left\langle\Psi_j\left|\sum_{p<q}V_{pq}\right|\Psi_{i_{\varepsilon_j}}\right\rangle\right|^2, \quad (6)$$

where $\Psi_{i_{\varepsilon_j}}$ is the ASF of a combined system of i and a free electron with energy ε_j. V_{pq} is the sum of the Coulomb and Breit operators, which in atomic units is expressed by[14]

$$V_{pq} = \frac{1}{r_{pq}} - \alpha_p\alpha_q\frac{\cos(\omega r_{pq})}{r_{pq}} + (\alpha_p\nabla_p)(\alpha_q\nabla_q)\frac{\cos(\omega r_{pq})-1}{\omega^2 r_{pq}}, \quad (7)$$

where α_p and α_q are the Dirac matrices, and ω is the wave number of the exchanged virtual photon.

In a practical calculation, the energies and the wavefunctions have been generated by a widely used atomic structure package GRASP92.[15] The ASF is a linear combination of the configuration state functions, which are antisymmetrized products of a common basis set of orthonormal orbitals. The basis set are optimized with respect to the Dirac–Coulomb Hamiltonian. Furthermore, the (transverse) Breit interactions are added by diagonalizing the Dirac–Coulomb–Breit Hamiltonian matrix. The dominant QED contributions, i.e. self-energy and vacuum polarization effects, are also included in the computations as perturbation. The radiative decay rates and the Auger decay rates are calculated by using the recently developed REOS99[12] and AUGER[13] programs respectively.

The DS strength S_{ijk} is obtained by integrating the DS cross-section $\sigma_{\rm DS}(i,j,k)$ in Eq.(1) over the energy ε in the vicinity of the resonance energy ε_j. Substituting Eqs.(3) and (4) into Eq.(2), we obtain

$$S_{ijk}(\varepsilon_j) = \frac{\pi^2\hbar^3}{m_{\rm e}\varepsilon_j}\frac{g_j}{2g_i}A^{\rm a}_{ji}\frac{A^{\rm r}_{jk}}{\Sigma_{k'}A^{\rm r}_{jk'}+\Sigma_{i'}A^{\rm a}_{ji'}}. \quad (8)$$

Then, the total DS cross-section $\sigma^{\rm DS}_t$ may be obtained by a sum of S_{ijk} over all the possible intermediate state j and the final state k. To facilitate $\sigma^{\rm DS}_t$ comparable with experiments on the scale of incident electron energy ε, we multiply a gaussian profile centred at ε_j with an energy resolution Γ to each S_{ijk}, we have

$$\sigma^{\rm DS}_t(\varepsilon) = \sum_{j,k}\frac{S_{ijk}(\varepsilon_j)}{\sqrt{2\pi}\Gamma}\exp\Big[-\frac{(\varepsilon-\varepsilon_j)^2}{2\Gamma^2}\Big]. \quad (9)$$

Here, the width is assumed to be 5 eV to get the detailed structure. Furthermore, to facilitate the total DS cross-section comparable with experiments on the scale of emitted photon wavelength λ, we may attach a Gaussian profile centred at a satellite line wavelength λ_{jk} with a width $\Delta\lambda$ to each S_{ijk}. We have $\sigma^{\rm DS}_\lambda(\lambda)$ as a function of λ, that is

$$\sigma^{\rm DS}_\lambda(\lambda) = \sum_{j,k}\frac{S_{ijk}(\lambda_{jk})}{\sqrt{2\pi}\Delta\lambda}\exp\Big[-\frac{(\lambda-\lambda_{jk})^2}{2\Delta\lambda^2}\Big]. \quad (10)$$

Here, the width $\Delta\lambda$ is given according to spectral resolution 2mÅ.

3. Result and discussion

We illustrate the convoluted DS cross-section $\sigma_t^{\rm DS}(\varepsilon)$ in Fig.1. In practical calculations, the $l_{\max}$ is assumed to be $(n-1)$ for the doubly excited states 1s2pnl ($n < 8$) and 6 for the doubly excited states 1s2pnl ($n > 7$). The resolved features are the emissions from KLM ($n = 3$), KLN ($n = 4$), KLO ($n = 5$), KLP ($n = 6$) and KLQ ($n = 7$) resonances. Even though they are unresolvable, the cross-sections up to $n = 10$ are also depicted in the figure. It can be seen that, although the strength of each resonance decreases as n increases, the resonances for large n ($n > 3$) give an important contribution. It amounts to 150% of the contribution from $n = 3$ resonance. And further on, in Table 1 we compared our results with previous data of the wavelengths[16,17] to verify the accuracy of the present calculation. It can be seen that our results are sound. We may conclude our that energies and hence our wavefunctions are sound.

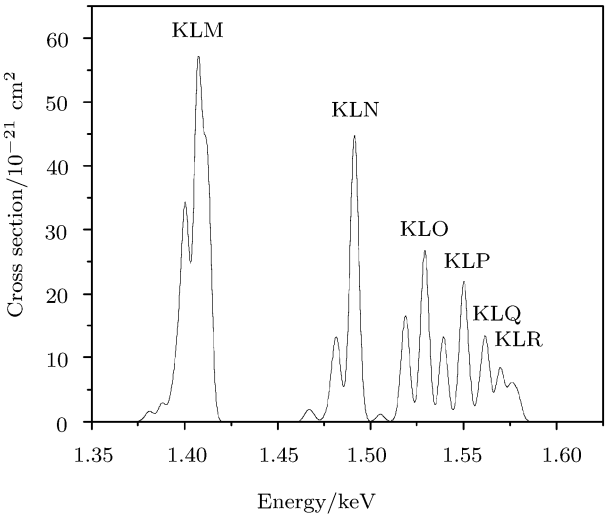


Fig.1. Calculated DS cross-sections as a function of electron energy for $n = 3$ to 10 resonances.

Table 1. Comparison of the present calculated DS wavelengths (in Å) of helium-like aluminium ions with available theoretical and experimental results.

lower level	upper level	$\lambda_{\rm thiswork}$	$\lambda_{\rm theor.}$	$\lambda_{\rm exp.}$
$1s^22s\ (0,1/2)_{1/2}$	$1s2s3p(1,3/2)_{3/2}$	6.7976	6.7952[16]	6.7926[17]
$1s^22s(0,1/2)_{1/2}$	$1s2s3p(1,3/2)_{1/2}$	6.7974	6.7950[16]	6.7915[17]
$1s^22s(0,1/2)_{1/2}$	$1s2s3p(0,1/2)_{1/2}$	6.7548	6.7499[16]	6.7464[17]
$1s^22s(0,1/2)_{1/2}$	$1s2s3p(0,3/2)_{3/2}$	6.7431	6.7490[16]	
$1s^22p(0,1/2)_{1/2}$	$1s2p3p(1,3/2)_{1/2}$	6.8303	6.8247[16]	
$1s^22p(0,3/2)_{3/2}$	$1s2p3p(1,3/2)_{1/2}$	6.8329	6.8284[16]	
$1s^22p(0,1/2)_{1/2}$	$1s2p3p(2,3/2)_{1/2}$	6.7984	6.7903[16]	
$1s^22p(0,3/2)_{3/2}$	$1s2p3p(2,3/2)_{1/2}$	6.8011	6.7940[16]	
$1s^22p(0,1/2)_{1/2}$	$1s2p3p(1,1/2)_{1/2}$	6.7857	6.7782[16]	
$1s^22p(0,3/2)_{3/2}$	$1s2p3p(1,1/2)_{1/2}$	6.7883	6.7818[16]	
$1s^22p(0,3/2)_{3/2}$	$1s2p3p(2,3/2)_{5/2}$	6.8130	6.8042[17]	6.8049[17]
$1s^22p(0,3/2)_{3/2}$	$1s2p3p(1,3/2)_{3/2}$	6.7859	6.7785[17]	6.7807[17]

In Fig.2, our three-dimensional dielectronic recombination (DR) spectrum is plotted to show a relationship between the DS strength and both the free-electron energy and DS wavelength. Here KLL resonances are not included because they deviate from Kα resonance line and are greater than 40mÅ, they give very small influence to the Kα resonance line. The notation $\lambda_{\rm K\alpha}$ is respectively the wavelength of Kα resonance line of helium-like aluminium ions. It can be seen that the resonance spectrum of $n = 3$ consists of two parts. Peak a is the contribution of 1s2p3d–$1s^23d$ transition, its mean wavelength is 7.767 Å. Peak b is the contribution of 1s2p3p–$1s^23p$ and 1s2p3s–$1s^23s$ transition, its mean wavelength is 7.781 Å. Because of the strong interaction between 2p and both 3s and 3p electrons, the difference between the mean wavelength of peak b and Kα resonance line is as large as 21mÅ. Every resonance spectrum of large n ($n > 3$) also con-

sists of two parts. Because the interaction between 2p and nl electrons becomes weaker with the increase of n value, the difference between two parts becomes smaller with the increase of n value.

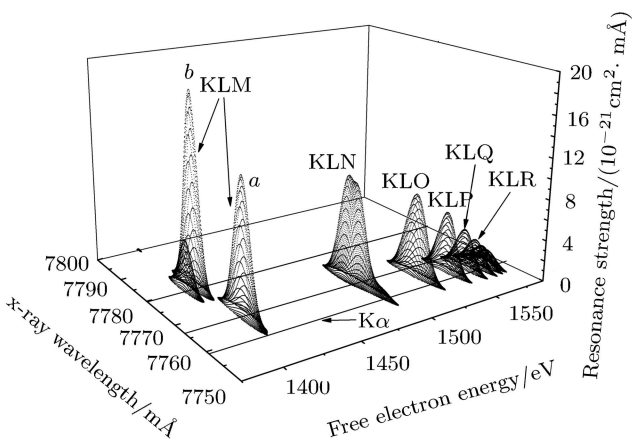


Fig.2. The three-dimensional plot of DR process of helium-like aluminium ions.

For showing the contributions of high-n DS to Kα resonance line in helium-like aluminium ions more clearly, we illustrate our calculated satellite line spectral contributions from various n as functions of wavelength deviation from Kα resonance line in Fig.3. Again peak 3a is the contribution from 1s2p3d–1s^{2}3d transition and peak 3b is contribution from 1s2p3p–1s^{2}3p and 1s2p3s–1s^{2}3s transition. Because of the large difference between peak 3b and Kα resonance line, the dominating contribution from KLM comes from peak 3a. The wavelength of Kα resonance line is 7.7597Å. We can see that the high-n satellites are found mostly on the long wavelength side, and their positions converge to the resonance line position as n ($n > 3$) increases. This means that these high-n DS lines are seriously superposed at the position of resonance line if they are existent in the plasma, which would lead to a significant increase in both the apparent width and the intensity of Kα resonance line. They also would induce a positional shift of Kα resonance line. In order to determine the total high-n contribution, $n_{\max} = 100$ has been chosen here. Of course, in a practical diagnostic application, $n_{\max}$ should be determined according to the practical plasma condition.[18]

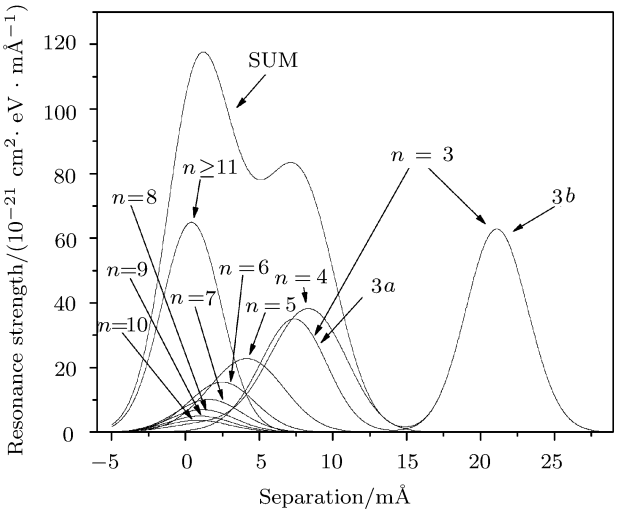


Fig.3. Calculated high-n DS resonance strengths as functions of deviation from Kα resonance line. The notation sum illustrates the sum of all the different n.

4. Conclusion

The DR cross-sections of helium-like aluminium ions have been studied in detail. It is found that the strength of each resonance decreases as n increases, the resonances for $n > 3$ give an important contribution. Even higher resonances for $n \geq 11$ cannot also be neglected.

The energy positions and strengths of the high-n satellites are presented also. As expected, they are always locating on the red wings, and approaching gradually to the resonance line and become weaker with the increase of n value. In this consequence, the accumulation of high-n DS lines can be very important for the results in a serious mixing with resonance line. Therefore, it is necessary to consider the contributions in a practical plasma diagnostic application. A comparison of the present theory with experiments will be an issue in coming papers.

References

[1] Bitter M, von Goeler S, Hill K W, Horton R, Johnson D, Roney W, Sauthoff N R, Silver E and Stodiek W 1981 *Phys. Rev. Lett.* **47** 921

[2] Bitter M, Hill K W, Zarnstorff M, von Goeler S, Hulse R, Johnson L C, Sauthoff N R, Sesnic S, Young K M, Tavernier M, Bely-Dubau F, Faucher P, Cornille M and Dubau J 1985 *Phys. Rev.* A **32** 3011

[3] Decaux V, Bitter M, Hsuan H, Hill K W, von Goeler S, Park H and Bhalla C P 1991 *Phys. Rev.* A **44** R6987

[4] Wang J G, Chang T Q, Dong C Z and Kato T 1999 *Eur.*

Phys. J. D **5** 167
[5] Nardi E and Zinamon Z 1981 *J. Appl. Phys.* **52** 7075
[6] Chen H, Soom B, Yaakobi B, Uchida S and Meyerhofer D D 1993 *Phys. Rev. Lett.* **70** 3431
[7] Hares J D, Kilkenny J D, Key M H and Lunney J G 1979 *Phys. Rev. Lett.* **42** 1216
[8] Jin Z and Zhang J 2000 *Acta Phys. Sin.* **50** 0365 (in Chinese)
[9] Djaoui A, Evans R, Hall T A, Badger A and Rosmej F B 1995 *J. Phys.* B **28** 1921
[10] Macfarlane J J, Wang P, Bailey J E and Mehlhorn T A 1999 *JQSRT* **61** 671
[11] Zhang D H, Dong C Z, Xie L Y, Ding X B and Fu Y B 2005 *Acta Phys. Sin.* **55** 112 (in Chinese)
[12] Fritzsche S, Fischer C F and Dong C Z 2000 *Comput. Phys. Commun.* **124** 340
[13] Fritzsche S, Aksela H, Dong C Z, Heinäsmäki S and Sienkiewicz J E 2003 *Nucl. Instr. Meth. Phys. Res.* B **205** 93
[14] Grant I P, Mckenzie B J and Norrington P H 1980 *Comput. Phys. Commun.* **21** 207
[15] Parpia F A, Fischer Froese C and Grant I P 1996 *Comput. Phys. Commun.* **94** 249
[16] Audebert P, Geindre J P, Gauthier C J, Alaterre Ph, Popovics C, Cornille M and Dubau J 1984 *Phys. Rev.* A **30** 1582
[17] Elliott S R, Beiersdorfer P, Libby S B, Osterheld A L and Phillips T 1994 *Opt. Commun.* **113** 204
[18] Griem H R 1997 *Principles of Plasma Spectroscopy* (Cambridge: Cambridge University Press)